Integration of On-The-Fly Kinetic Reduction with Multidimensional CFD

Kaiyuan He, Marianthi G. Ierapetritou, and Ioannis P. Androulakis
Dept of Chemical and Biochemical Engineering, Rutgers, The State University of New Jersey, Piscataway, NJ 08854

DOI 10.1002/aic.12072
Published online September 29, 2009 in Wiley InterScience (www.interscience.wiley.com).

A reduction approach for coupling complex kinetics with engine computational fluid dynamics (CFD) code has been developed. An on-the-fly reduction scheme was used to reduce the reaction mechanism dynamically during the reactive flow calculation in order to couple comprehensive chemistry with flow simulations in each computational cell. KIVA-3V code is used as the CFD framework and CHEMKIN is employed to formulate chemistry, hydrodynamics and transport. Mechanism reduction was achieved by applying element flux analysis on-the-fly *in the context of the multidimensional CFD calculation. The results show that incorporating the on-the-fly reduction approach in CFD code enables the simulation of ignition and combustion process accurately compared with detailed simulations. Both species and time-dependant information can be provided by the current model with significantly reduced CPU time*. © 2009 American Institute of Chemical Engineers *AIChE J,* 56: 1305–1314, 2010
Keywords: on-the-fly reduction, CFD, detailed kinetics

Introduction

As the increase of computational capability in recent years, more accurate computational fluid dynamics (CFD) models have been developed. The fundamental basis of any CFD model is the solution of Navier-Stokes equations.[1] Further complicating factors are that the flow occurs in a complex geometry, the incorporation of turbulence, and the integration of detailed chemical kinetics. To describe turbulence several models have been developed such as direct numerical simulation (DNS) method[2] and k-ε model.[3] In recent years much progress has been made in CFD model development for engines. For example, studies have been conducted for direct-injection diesel engines,[4,5] indirect-injection diesel engines,[6] stratified-charge rotary engines,[7] and homogeneous-charge compression ignition engines.[8,9] Although these engine simulation codes are comprehensive and can predict engine details to some extent, they are not entirely predictive for the combustion process due to the wide range of combustion time scales and engine conditions. Thus, submodels have been developed to capture the short time scale processes such as drop vaporization[10–12] and turbulence dispersion.[13,14] A detailed review of CFD packages and their capability is given in.[15]

CFD code packages have been developed to include both the fluid dynamics models and these complementary submodels for engine simulation. However, most of these packages are for commercial use and the source codes are generally not available. In this study, KIVA code[16] has been selected as the engine model, since it is one of the most commonly used CFD packages and has the ability to calculate three-dimensional (3-D) flows in engine cylinders, arbitrary piston shapes, and capture the effects of turbulence and heat gradients near walls. The package has been widely used in engine simulations to predict ignition and combustion process.[17–19] The more essential factor is that the source code of KIVA is accessible and thus it can be used in model development work as a test bed.[17] Given the model's capability to capture detailed flow properties, it has also been widely recognized that incorporating detailed chemistry in CFD calculation to describe a reactive flow is necessary. The realization of this has motivated continuing development of CFD

Correspondence concerning this article should be addressed to I. P. Androulakis at yannis@rci.rutgers.edu

© 2009 American Institute of Chemical Engineers

hand-in-hand with a corresponding development of detailed fundamental kinetic models consisting of hundreds of species and thousands of reactions. However, the integration of detailed kinetic mechanisms in CFD calculation often consumes extremely long CPU time due to the large system of nonlinearly coupled stiff ordinary differential equations (ODE) system. Previous studies have demonstrated that even with mechanisms with species less than 50, over 90% of the CPU time was consumed in solving the ODE systems in reactive flow calculation.[20,21]

To integrate comprehensive chemistry in fluid calculation without introducing too much computational intensity, several methodologies have been proposed which generally fall in three categories: skeletal mechanism reduction, adaptive reduction, and on-the-fly reduction. Skeletal mechanism reduction approaches develop a global reduced mechanism to define the entire simulation. This category includes the redundant species identification and sensitivity analysis approaches proposed by Turanyi[22] and Rabitz,[23] the quasi-steady-state-assumption (QSSA) and partial equilibrium approximations,[24,25] the intrinsic low-dimensional manifolds (ILDM),[26] the computational singular perturbation (CSP),[27,28] the direct-relation-graph (DRG) method,[29–31] the optimization-based mathematical programming approach,[32–34] and the element flux analysis based approach.[35] However, a global mechanism cannot be always accurate for various conditions that are confronted in a reactive flow. Thus, adaptive kinetic reduction strategy has been explored to use different mechanisms for different conditions. Several adaptive schemes have been proposed such as *in situ* adaptive tabulations (ISAT),[36] the "store and retrieve" approach,[37] and the reduction scheme subject to the validity of temperature, pressure, and species compositions.[38,39] In our previous work, an adaptive framework was developed based on flux graph analysis and clustering algorithms.[40] Adaptive reduction approaches are more accurate than globally reduced mechanisms; however, they rely on the development of a library of reduced mechanisms which requires priori analysis of the simulations. Due to the wide range of conditions encountered in chemical systems, the union of the feasible regions of reduced mechanisms in the library may not cover all possible reactive conditions. This deficiency has led some researchers to explore on-the-fly reduction methodologies which do not rely on *a priori* analysis. The on-the-fly reduction schemes analyze local reactive conditions and dynamically develop reduced mechanisms which are locally accurate during the reactive flow simulation. Liang et al.[19] proposed an on-the-fly approach based on the direct relation graph method.[29–31] In our previous work, an on-the-fly reduction scheme based on the element flux analysis was proposed. The element flux analysis was first introduced by Revel et al.[41] and was implemented in mechanism reduction by Androulakis et al.[35] The carbon flux between reacting species are calculated at each simulation time step and sorted in descending order. By setting a user-selected cutoff value, active species with large element flux can be identified, which constitute the local reduced mechanism to define the chemistry at this particular time step. No *a priori* analysis or information is needed for this approach, and the active species can be identified effectively without extensive computational overhead.

In our previous work, reactor models with simple geometry have been used to validate the on-the-fly reduction methodology. However, it is necessary to further validate the reduction scheme in a multi-dimensional CFD model which simulates hydrocarbon fuel combustion in more realistic engines. Thus, in this work, the on-the-fly reduction scheme is integrated in the framework of KIVA-3V[16] using a 2-D numerical mesh with moving boundaries which simulates homogeneous charge compression ignition (HCCI) combustion. The on-the-fly reduction scheme is applied to each computational cell at each time step and reduced mechanisms are generated dynamically to describe the local chemistry.

Element flux analysis and on-the-fly reduction scheme

The mechanism reduction methodology used in this work is based on the hypothesis that the element flux can depict the reactive propensity more accurately than mass fraction T and P. The element flux analysis, first introduced by Revel et al.[41] provides a pointer which quantifies the activity of sources and sinks in a reaction system. The instantaneous elemental flux of atom A from species j to species k through reaction i, denoted as A_{ijk}, was defined as Eq. 1 in Revel's article. A_{ijk} has the same sign as the net reaction rate $q_i(t)$, in other words, A_{ijk} is positive if the reaction is shifting in the direction from specie j to k and negative from k to j. The total instantaneous flux from specie j to specie k can be calculated by summing A_{ijk} over all the reactions in which species j and k are involved, as represented in Eq. 2

$$\dot{\mathrm{A}}_{ijk}(t) = q_i(t)\frac{n_{A,j}n_{A,k}}{N_{A,i}} \tag{1}$$

$$\overline{\dot{\mathrm{A}}}_{jk}(t) = \sum_{i=1}^{N_R} \dot{\mathrm{A}}_{ijk}(t) \tag{2}$$

where $q_i(t)$ is instantaneous rate of reaction i (mol/s), $n_{A,j}$ is the number of atoms A in species j, $n_{A,k}$ is the number of atoms A in species k, $N_{A,i}$ is the total number of atoms A in reaction i, and N_R represents the number of reactions that these species participate as reactants or products. However, Eqs.1 and 2 may result in information loss when quasi-steady-state species or partial equilibrium reactions exit. For quasi-steady-state species, flux in is defined to be positive while flux out is negative. When the net flux is calculated in Eq. 2, flux in and flux out will cancel each other which results in a small net flux. Similar problem might stem from the existence of partial equilibrium reactions. For partial equilibrium reactions, their large forward and reverse reaction rates may result in a small net reaction rate, which is the $q_i(t)$ used to evaluate A_{ijk} in Eq.1. To avoid information loss when addressing quasi-steady-state species and partial equilibrium reactions, both the forward and reverse reactions rates should be taken into account separately when calculating flux. Eq.1 has been thus improved to the following form

$$\dot{\mathrm{A}}_{ijk}(t) = (|q_{ifwd}(t)| + |q_{irev}(t)|)\frac{n_{A,j}n_{A,k}}{N_{A,i}} \tag{3}$$

where q_{ifwd} and q_{irev} are the reactions rates of forward and reverse reactions, respectively. The absolute values of both

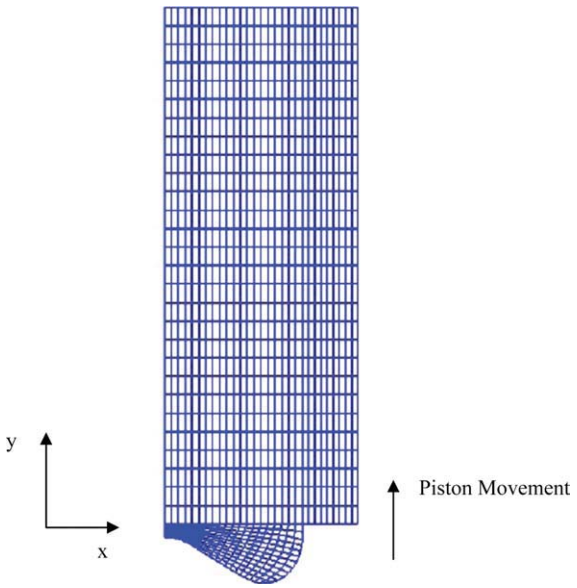

Figure 1. Numerical mesh of KIVA-3V used in this study.

[Color figure can be viewed in the online issue, which is available at www.interscience.wiley.com.]

forward and reverse reaction rates can ensure no significant information loss when evaluating element flux for both partial equilibrium reactions and quasi-steady-state species. To clarify the way the calculation are implemented we have provided in Appendix I a section of our FORTRAN implementation of flux code, where we follow a standard CHEMKIN notation. The flux is estimated at every time step (IT). The maximum number of FROM - TO species pairs that have element transfer is $N_{species} \times N_{species}$. However, not every pair is connected in the mechanism. To avoid unnecessary CPU time on looping over species pairs that are not connected, a loop over all reactions (NII) is employed instead of a two-level loop over all species ($N_{species} \times N_{species}$).

To develop locally accurate reduced mechanisms for different reactive conditions, all non-zero element flux pointers AJK at each time step are sorted in a descending order. Then a user-selected cutoff value is applied on the flux. Only species above the cutoff which are characterized by relatively larger flux are retained in the reduced mechanism.

Having determined an efficient scheme for obtaining reduced mechanisms based on flux analysis, the next step is to integrate the reduction scheme in reactive flow simulation. Based on the reduced species set identified in the flux analysis, a reduced mechanism is generated *on-the-fly* using the CHEMKIN application. The concentrations of species in the

Table 1. Engine Parameters and Operating Conditions

Parameter	Value
Engine speed	700 rpm
Compression ratio	16:1
Fuel	n-pentane
Start of calculation	−40
Initial pressure	5 bar
Equivalence ratio	1.0

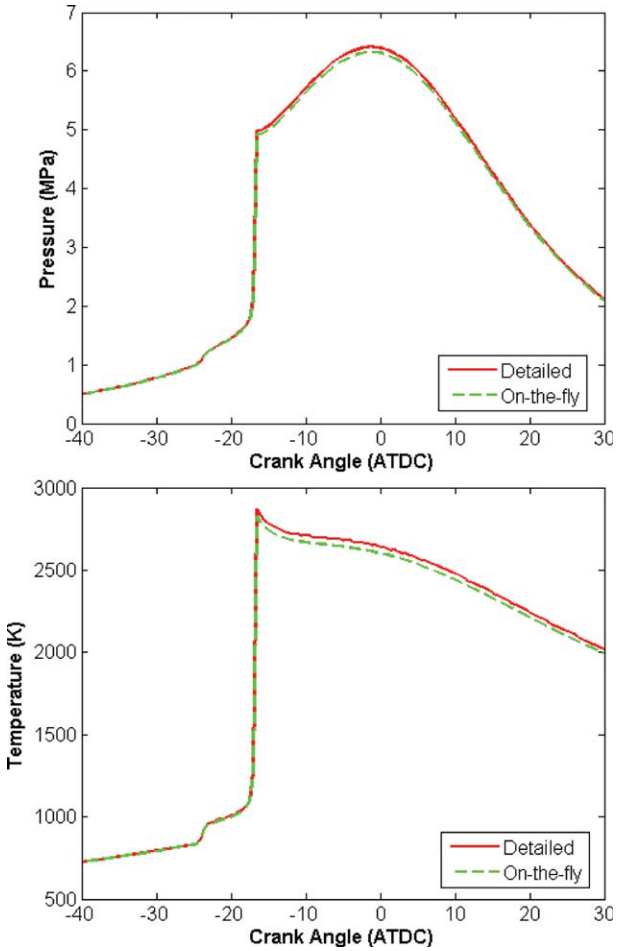

Figure 2. In-cylinder pressure and temperature profiles of n-pentane combustion in KIVA simulation at 725 K and 5 bar.

[Color figure can be viewed in the online issue, which is available at www.interscience.wiley.com.]

reduced mechanism are then integrated, while the species that are not included in the reduced mechanism are considered as dormant (to have zero production rates) at current time step. Their concentrations are kept unchanged in the main function and are not integrated in CHEMKIN application. Therefore, substantial CPU time can be saved on integrating dormant species. As the system advances to next time step, the flux analysis and reduction process are recalled and a new reduced mechanism is generated. Compared to adaptive reduction schemes, which construct a library of reduced mechanisms *a priori* and assume the union of feasible regions of these mechanisms covers the entire condition space encountered in the simulation, the main advantage of dynamic mechanism generation is that, accurate mechanisms can be developed based on local reactive conditions.

Demonstration of the on-the-fly scheme in KIVA-3V

To validate the proposed on-the-fly reduction scheme, a detailed n-pentane oxidization mechanism consists of 385 species and 1895 reactions[42] is used in KIVA-3V. KIVA-3V

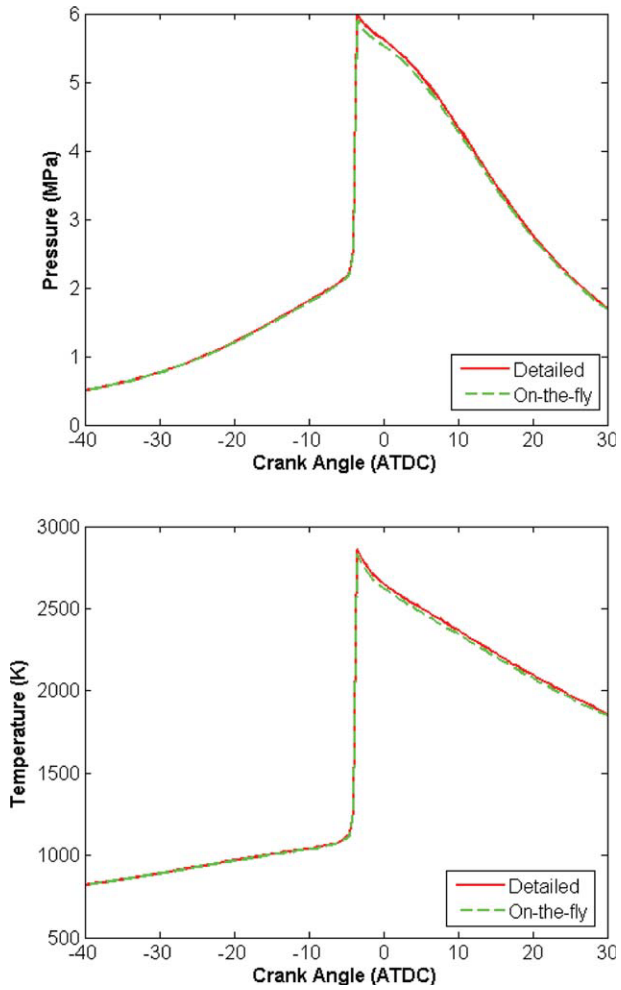

Figure 3. In-cylinder pressure and temperature profiles of n-pentane combustion in KIVA at 820 K and 5 bar.

[Color figure can be viewed in the online issue, which is available at www.interscience.wiley.com.]

handles the fluid mechanical processes on a highly resolved mesh grid. For 2-D simulation of HCCI engines, the challenge for mesh generation is its geometry complexity and moving piston and valves. Since the HCCI engine combustion is mainly controlled by chemical kinetics, only the temperature gradient near the engine walls and pistons are taken into account in the present study. In order to provide high enough resolution to describe the geometry of the HCCI engine, and meanwhile keep the computation task accessible to current computers, a 2-D numerical mesh which has approximately 1,000 cells at bottom dead center (BDC) position is generated for the simulation, as shown in Figure 1. All the cells are sorted so that deactivated cells are placed at the beginning of the cell computational vector followed by active cells. The calculation only loops over all active cells. By doing this sort, the mesh is block-structured and thus eliminates the necessity of maintaining large regions of deactivated cells and results in a reduction of both storage and computer time for complex geometries. To demonstrate that the proposed on-the-fly scheme is able to capture the reactive propensity of the system, KIVA simulations were monitored from −40 to 30 after top dead center (ATDC). System temperatures at −40 ATDC are chosen as 725 K, 820 K, and 1000 K to represent low, intermediate, and high-temperature combustion, respectively. Typical HCCI operations starting from −180 ATDC at 300 K to 450 K will heat the cylinder to the range of 700 K to 900K when piston reaches −40 ATDC.[43,44] The simulations in this work were monitored from −40 ATDC to 30 ATDC because the major part of combustion occurs in this range and simulations of the full compression process (from −180 ATDC to 180 ATDC) would require substantially more CPU time. Detailed engine parameters and run conditions are listed in Table 1.

Results of the on-the-fly scheme have been compared with simulations using the detailed mechanism. The detailed mechanism consists of 385 species and 1,895 elementary reactions. The average size of reduced mechanisms generated in the on-the-fly reduction is 82 species and 451 elementary reactions. Figures 2–4 illustrate pressure and temperature profiles of HCCI operations with 725 K, 820 K, and

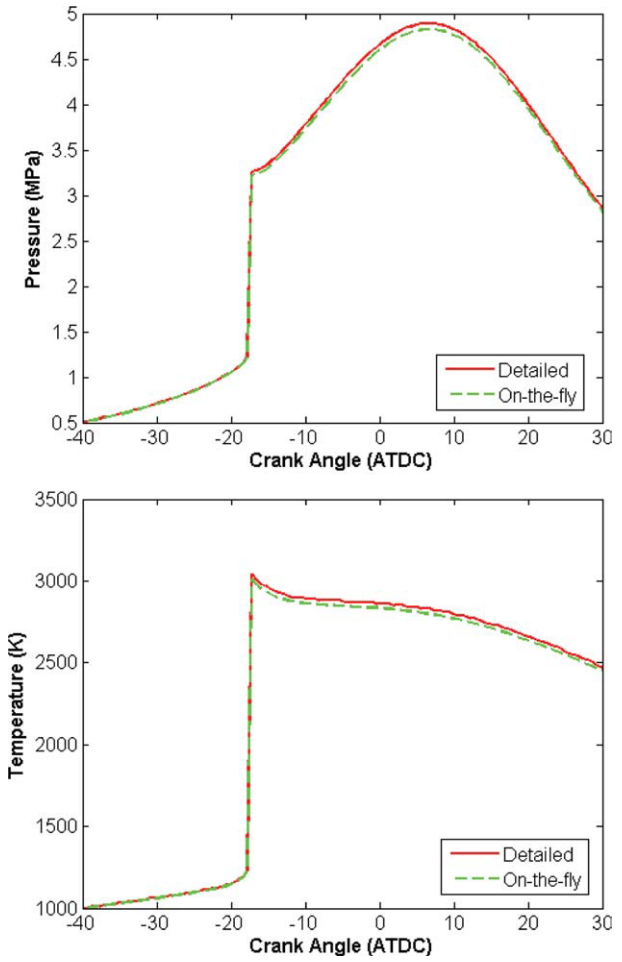

Figure 4. In-cylinder pressure and temperature profiles of n-pentane combustion in KIVA at 1000 K and 5 bar.

[Color figure can be viewed in the online issue, which is available at www.interscience.wiley.com.]

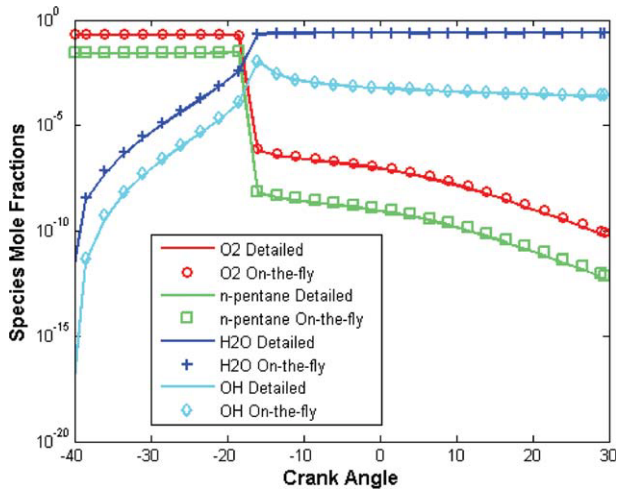

Figure 5. Species mass fractions of n-pentane combustion in KIVA at 1000 K and 5 bar.

Lines represent the detailed simulation and markers represent the on-the-fly simulation. [Color figure can be viewed in the online issue, which is available at www.interscience.wiley.com.]

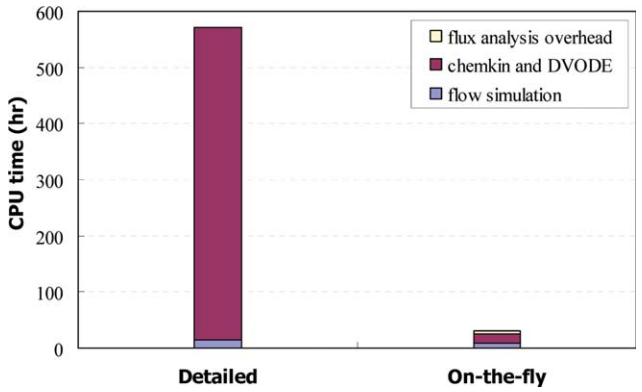

Figure 6. CPU time distribution of detailed simulation and on-the-fly scheme of n-pentane combustion in KIVA.

[Color figure can be viewed in the online issue, which is available at www.interscience.wiley.com.]

1000 K at −40 ATDC, respectively. As shown in the pressure and temperature profiles, both the ignition timing and the peak pressure are well predicted by the on-the-fly scheme. Since the on-the-fly scheme dynamically develops accurate mechanisms for local conditions, at each time step a small mechanism is capable to capture most of the reactive propensity of the system. Thus although the average size of mechanisms in the on-the-fly simulation are small compared to the detailed mechanism, excellent accuracy can be achieved.

Concentration histories of fuel, oxidizer, OH radical, and product H_2O are compared with detailed simulation in Figure 5, which also showed encouraging agreement and further validated the effectiveness of the on-the-fly scheme. CPU times for the on-the-fly reduction scheme and the detailed simulation are compared in Figure 6. Three factors are represented in the figure: (1) the overhead introduced by the flux analysis and mechanism reduction; (2) CPU time for chemical kinetics calculation; and (3) CPU time for flow calculation. As we can see from the detailed simulation, more than 90% of the total CPU time was spent on resolving the chemistry part. Using the on-the-fly simulation, the CPU time spent for the chemistry part was significantly reduced while flow calculation was comparable with the detailed simulation. The overhead introduced by the flux analysis and mechanism reduction comprises less than 5% of the total CPU time of the on-the-fly simulation. By comparing the CPU times on all these parts, the on-the-fly scheme reduced the chemistry calculation by a factor of 30 and the overall CPU time by a factor of 20.

The general information such as temperature and pressure profile is not able to represent the detailed pathways, thus, some species-dependent and time-dependent information are needed to get a comprehensive picture of the combustion process. Considering the n-pentane oxidation for example, as shown in Figure 7 the ignition follows different pathways under different operating conditions. To depict the activity level of different pathways, three species are monitored in the simulation: the radical after the second oxygen addition $C_5H_{10}OOH1\text{-}3O_2$ to represent the low-temperature oxidation pathway, the epoxide $C_5H_{10}O1\text{-}3$ to represent the intermediate temperature oxidation pathway, and the olefin C_3H_6 to indicate the high-temperature beta-scission pathway. Distribution patterns of temperature and these key species in the cylinder at 725 K, 820 K, and 1000 K are illustrated in Figures 8–10. In Figures 8–10, the x and y axis are the two dimensions of the numerical mesh of the KIVA model, while z axis represents the temperature or species mole fractions. As shown from the temperature and species distribution profiles, at 725 K the radical $C_5H_{10}OOH1\text{-}3O_2$ reaches a high level and goes through similar evolution patterns as

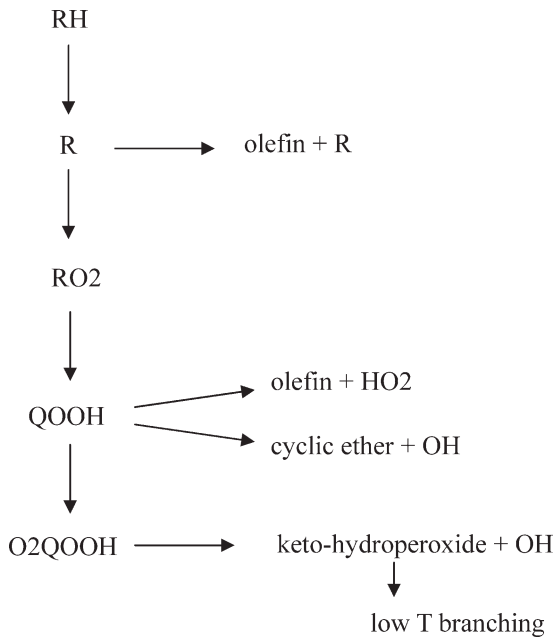

Figure 7. Primary oxidation pathways of n-pentane combustion.

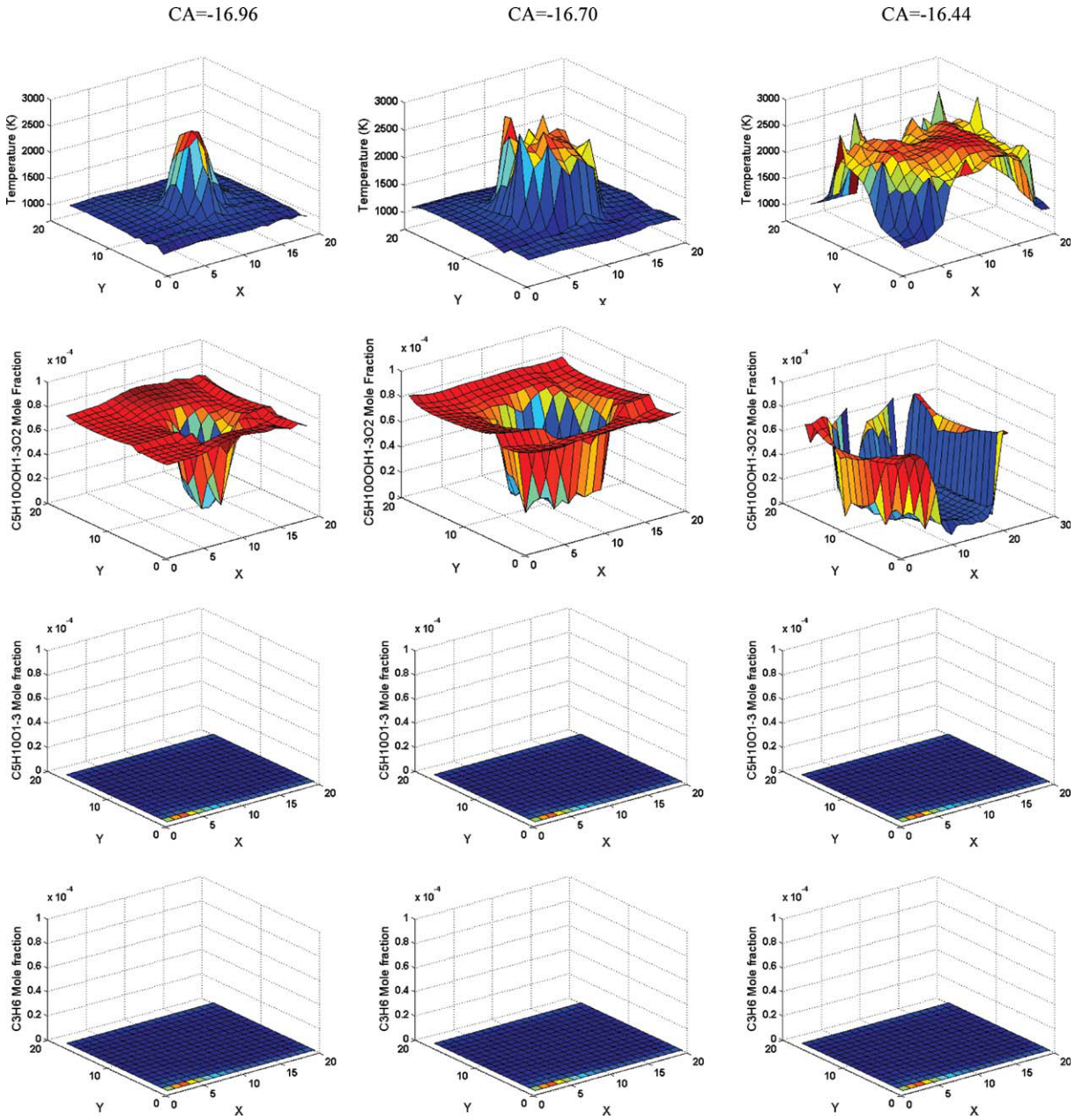

Figure 8. Evolution patterns of typical species of different pathways compared with n-cylinder temperature profile.

The first column represents crank angle −16.96 degree, the second column represents crank angle −16.70 degree, and the third column represents crank angle −16.44 degree. X and Y axis represent the cell index of the numerical mesh as shown in Figure 1. Initial conditions: T = 725 K, P = 5 bar. [Color figure can be viewed in the online issue, which is available at www.interscience.wiley.com.]

the ignition propagates. Meanwhile, $C_5H_{10}O1\text{-}3$ and C_3H_6 are kept at a low level. Similar correlations can be observed at the intermediate temperature (820 K) ignition, where $C_5H_{10}O1\text{-}3$ is highly active while $C_5H_{10}OOH1\text{-}3O_2$ and C_3H_6 demonstrate a low activity. At high-temperature (1000 K), beta-scission pathway dominates the oxidation, thus C_3H_6 is active while $C_5H_{10}OOH1\text{-}3O_2$ and $C_5H_{10}O1\text{-}3$ is not accumulated. The typical species have different activity levels at different ignition conditions. By tracking species in the system, the proposed approach can provide species-dependant and time-dependant information of specific interest, which is usually not available in conventional experiments and simulations with simplified chemical kinetics.

Conclusions

The on-the-fly mechanism reduction methodology based on element flux analysis has been validated in an HCCI engine model in KIVA-3V. Excellent agreement on temperature, pressure and species compositions was observed between the on-the-fly simulation and the detailed simulation. Varying sizes of reduced mechanisms were generated based on local reaction condition and the CPU time was reduced by

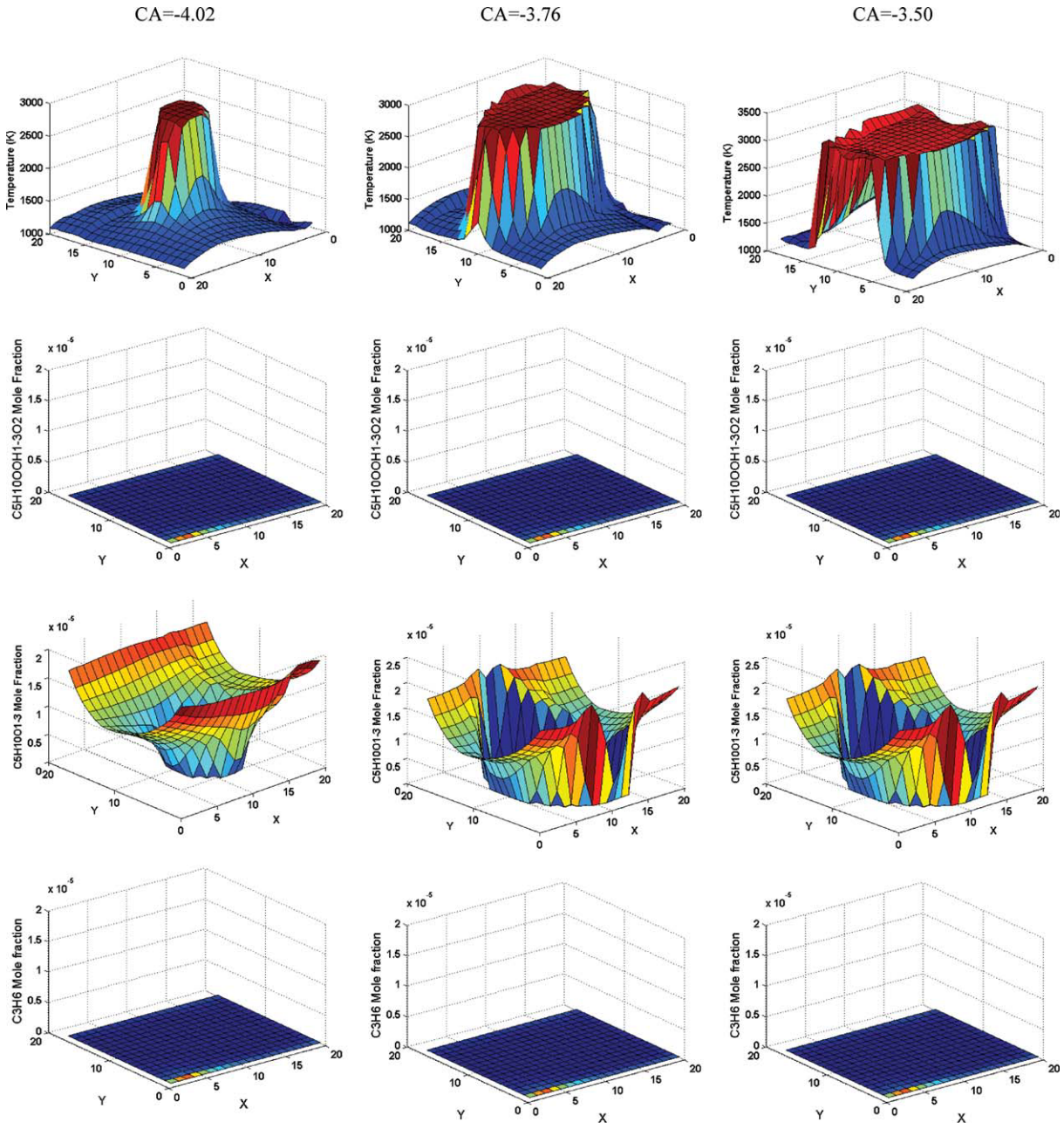

Figure 9. Evolution patterns of typical species of different pathways compared with in-cylinder temperature profile.

The first column represents crank angle −4.02 degree, the second column represents crank angle −3.76 degree, and the third column represents crank angle −3.50 degree. X and Y axis represent the cell index of the numerical mesh as shown in Figure 1. Initial conditions: T = 820 K, P = 5 bar. [Color figure can be viewed in the online issue, which is available at www.interscience.wiley.com.]

20-fold. The results from n-pentane combustion in engine simulation have demonstrated that integrating the on-the-fly scheme in CFD model provides a powerful tool to illustrate detailed species-dependant and time-dependant information about fuel combustion, of particular importance is complex fuels for which simulation using detailed mechanism is computationally too expensive. Thus, the on-the-fly reduction scheme shows great potential in providing accurate virtual experimental environment for complex fuel combustions with moderate CPU time.

In the methodology developed so far, the on-the-fly scheme develops reduced mechanisms based on the full array of species composition and system temperature and pressure, thus for any typical combustion simulations, using either 0-dimensional reactor model or a multi-dimensional CFD model, the reduction scheme can be integrated in the calculation with negligible computational overhead. The methodology also provides a user-selected cutoff value used in the flux analysis; this tunable value enables users to compromise between the level of accuracy and the computational

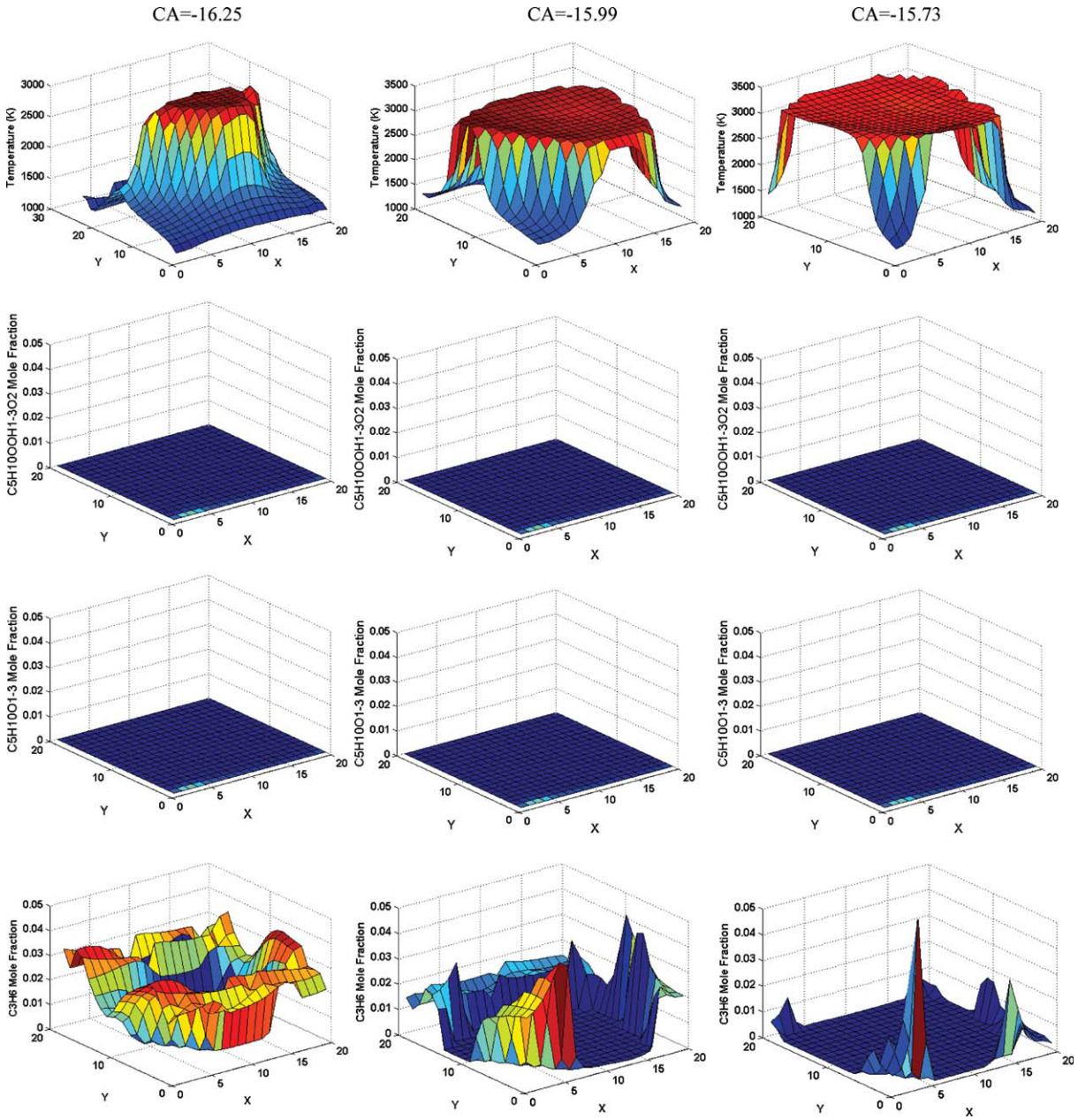

Figure 10. Evolution patterns of typical species of different pathways compared with in-cylinder temperature profile.

The first column represents crank angle −16.25 degree, the second column represents crank angle −15.99 degree, and the third column represents crank angle −15.73 degree. X and Y axis represent the cell index of the numerical mesh as shown in Figure 1. Initial conditions: T = 1000 K, P = 5 bar. [Color figure can be viewed in the online issue, which is available at www.interscience.wiley.com.]

complexity. In the cases where accuracy is the first priority, higher cutoff will be appropriate, while in the systems where computational intensity is the biggest obstacle, lower cutoff will ensure integrating comprehensive chemistry using less CPU time.

Acknowledgments

The authors gratefully acknowledge Long Liang, John G. Stevens, and John T. Farrell from ExxonMobil Research and Engineering Co. for very useful discussions. Also, the authors thank the financial support from ExxonMobil Corporation, NSF CBET Grant 0730582, and ONR Contract N00014-06-10835.

Literature Cited

1. Hirschfelder JO, Curtiss CF. In: *Theory of propagation of flames*. 3rd Symp. Comb, Flame and Explosion Phenomena, Baltimore: 1949;121.
2. Reynolds WC. The potential and limitations of direct and large eddy simulation. *Lecture Notes in Physics*. 1989;313.
3. Jones WP, Whitelaw JH. In: *Modelling and measurement in turbulent combustion*, 20th Symp Comb, Pittsburgh, 1985; Pittsburgh, PA: 1985;223.

4. Hou Z-X, Abraham J. Three-dimensional modeling of soot and NO in a direct-injection diesel engine. *Society of Automotive Engineers Technical Paper 950608*, 1995.
5. Patterson MA, Kong S-C, Hampson GJ, Reitz RD. Modeling the effects of fuel injection characteristics on diesel engine soot and NOx emissions. *Society of Automotive Engineers Technical Paper 940523*; 1994.
6. Scheimer GW, Strauss TS, Ritschder U. Combustion in a swirl chamber diesel engine simulation by computational fluid dynamics. *Society of Automotive Engineers Technical Paper 950280*; 1995.
7. Abraham J, Bracco FV. Fuel-air mixing and distribution in a direct-injection stratified-charge rotary engine. *Society of Automotive Engineers Technical Paper 890329*, 1989.
8. Aceves SM, Flowers DL, Westbrook CL, Smith JR, Pitz W, Dibble R, Christensen M, Johansson B. A Multi-zone Model for Prediction of HCCI Combustion and Emissions. *SAE paper 2000–01-0327*; 2000.
9. Babajimopoulos A, Assanis DN, Flowers DL, Aceves SM, Hessel RP. In: *A Fully Integrated CFD and Multi-zone Model with Detailed Chemical Kinetics for the Simulation of PCCI Engines*. 15th International Multidimensional Engine Modeling Users' Group Meeting, 2005; Detroit, MI: 2005.
10. Marchese AJ, Dryer FL, Nayagam V. Numerical modeling of isolated n-alkane droplet flames: Initial comparisons with ground and space-based microgravity experiments. *Combust Flame*. 1999; 116(3):432–459.
11. Sirignano WA. Fluid-dynamics of sprays—1992 Freeman Scholar lecture. *J Fluids Eng-Trans Asme*. 1993;115(3):345–378.
12. Chiang CH, Raju MS, Sirignano WA. Numerical-analysis of convecting, vaporizing fuel droplet with variable properties. *Int J Heat Mass Transfer*. 1992;35(5):1307–1324.
13. Mashayek F. Direct numerical simulations of evaporating droplet dispersion in forced low Mach number turbulence. *Int J Heat Mass Transfer* 1998;41(17):2601–2617.
14. Squires KD, Eaton JK. Measurements of particle dispersion obtained from direct numerical simulations of isotropic turbulence. *J Fluid Mech*. 1991;226:1–35.
15. Rumsey CL, Ying SX. Prediction of high lift: review of present CFD capability. *Prog Aerosp Sci*. 2002;38(2):145–180.
16. Amsden AA. KIVA-3V: A Block-Structured KIVA Program for Engines with Vertical or Canted Valves. *Los Alamos National Laboratory Report LA-13313-MS*, 1997.
17. Kong SC, Marriott CD, Reitz RD, Christensen M. Modeling and Experiments of HCCI Engine Combustion Using Detailed Chemical Kinetics with Multi-dimensional CFD. *SAE paper 2001-01-1026*; 2001.
18. Kong SC, Ayoub NA, Reitz RD. Modeling Combustion in Compression Ignition Homogeneous Charge Engines. *SAE paper 920512*, 1992.
19. Liang L, Stevens JG, Farrell JT. A dynamic adaptive chemistry scheme for reactive flow computations. *Proc Combust Inst*. 2009; 32:527–534.
20. Liang L, Kong SC, Jung C, Reitz RD. Development of a semi-implicit solver for detailed chemistry in internal combustion engine simulations. *J Eng Gas Turbines Power*. 2007;129(1):271–278.
21. Tones SR, Moriarty NW, Frenklach M, Brown NJ. Computational economy improvements in PRISM. *Int J Chem Kinetics*. 2003; 35(9):438–452.
22. Turanyi T. Reduction of large reaction mechanisms. *New J Chem.* 1990;14:795–803.
23. Rabitz H, Kramer M, Dacol D. Sensitivity analysis in chemical kinetics. *Annu Rev Phys Chem.* 1983;34:419–461.
24. Chen JY. A general procedure for constructing reduced reaction mechanisms with given independent reactions. *Combust Sci Tech.* 1988;57:89–94.
25. Peters N. In: *Systematic reduction of flame kinetics - Principles and details*. 11th International Colloquium on Dynamics of Explosions and Reactive Systems; 1988: Warsaw, Poland. 1988;67–86.
26. Mass U, Pope SB. Simplifying chemical kinetics: Intrinsic low dimensional manifold in composition space. *Combusti Flame*. 1992; 88:239–264.
27. Lam SH, Goussis DA. The Csp method for simplifying kinetics. *Int J Chem Kinetics*. 1994;26(4):461–486.
28. Lu TF, Ju YG, Law CK. Complex CSP for chemistry reduction and analysis. *Combust Flame*. 2001;126(1–2):1445–1455.
29. Lu TF, Law CK. A directed relation graph method for mechanism reduction. *Proc Combust Inst*. 2005;30:1333–1341.
30. Lu TF, Law CK. Linear time reduction of large kinetic mechanisms with directed relation graph: n-Heptane and iso-octane. *Combust Flame*. 2006;144(1–2):24–36.
31. Lu TF, Law CK. On the applicability of directed relation graphs to the reduction of reaction mechanisms. *Combust Flame*. 2006;146(3): 472–483.
32. Androulakis IP. Kinetic mechanism reduction based on an integer programming approach. *AIChE J*. 2000;46(2):361–371.
33. Bhattacharjee B, Schwer DA, Barton PI, Green WH. Optimally-reduced kinetic models: reaction elimination in large-scale kinetic mechanisms. *Combust Flame*. 2003;135(3):191–208.
34. Petzold L, Zhu WJ. Model reduction for chemical kinetics: An optimization approach. *AIChE J*. 1999;45(4):869–886.
35. Androulakis IP, Grenda JM, Bozzelli JW. Time-integrated pointers for enabling the analysis of detailed reaction mechanisms. >*AIChE J*. 2004;50(11):2956–2970.
36. Pope SB. Computationally efficient implementation of combustion chemistry using in situ adaptive tabulation. *Combust Theor Model*. 1997;1(1):41–63.
37. Androulakis IP. "Store and retrieve" representations of dynamic systems motivated by studies in gas phase chemical kinetics. *Comput Chem Eng*. 2004;28(11):2141–2155.
38. Banerjee I, Ierapetritou MG. Development of an adaptive chemistry model considering micromixing effects. *Chem Eng Sci*. 2003;58(20): 4537–4555.
39. Schwer DA, Lu PS, Green WH. An adaptive chemistry approach to modeling complex kinetics in reacting flows. *Combust Flame*. 2003; 133(4):451–465.
40. He K, Ierapetritou MG, Androulakis IP. A graph-based approach to developing adaptive representations of complex reaction mechanisms. Combust Flame. 2008;155(4):585–604.
41. Revel J, Boettner JC, Cathonnet M, Bachman JS. Derivation of a global chemical kinetic mechanism for methane ignition and combustion. *J Chim Phys Phys-Chim Biol*. 1994;91(4):365–382.
42. Curran HJ, Gaffuri P, Pitz WJ, Westbrook CK. A comprehensive modeling study of n-heptane oxidation. *Combust Flame*. 1998; 114(1–2):149–177.
43. Kong SC, Reitz RD. Numerical study of premixed HCCI engine combustion and its sensitivity to computational mesh and model uncertainties. *Combust Theor Model*. 2003;7(2):417–433.
44. Kong SC, Reitz RD. Application of detailed chemistry and CFD for predicting direct injection HCCI engine combustion and emissions. *Proc Combust Inst*. 2003;29:663–669.

Appendix I. Pseudo Code of Element Flux Analysis

Species participating in each reaction (K and K1) are identified, and if two species contain the element of interest (pseudo code line 4 and line 8), we use the stoichiometric coefficients ISTOIC and ISTOIC1 to determine whether the two species have a reactant/product relationship (pseudo code line 10). Then the summation of the absolute values of forward and reverse reaction rates and number of atoms of element NELE in species K and K1, and this specific reaction determine the flux value between these two species (pseudo code line 15 and 16). The flux pointer for the two species AJK(IFROM, ITO) of current time step is created and stored.

- ICWKR: CHEMKIN work array containing all necessary information for describing the reactions and the associated thermodynamics
- NII: number of reactions in the mechanism
- MXSP: maximum species allowed per reaction
- ICNK: memory location defined by CHEMKIN

- ISTOIC: stoichiometirc coefficient
- NCF: CHEMKIN function determining whether species ''K'' contains element ''NELE''
- Qfwd: array containing forward reaction rate calculated internally via CHEMKIN
- Qrev: array containing reverse reaction rate calculated internally via CHEMKIN

```
 1 DO I = 1, NII
 2 DO N = 1, MXSP-1
 3 K = ICKWRK(ICNK + (I-1)*MXSP + N − 1)
 4 IF (K .NE. 0 .AND. NCF(NELE,K) .GT. 0) THEN
 5 ISTOIC = ICKWRK(ICNU + (I-1)*MXSP + N − 1)
 6 DO N1 = N+1, MXSP
 7 K1 = ICKWRK(ICNK + (I-1)*MXSP + N1 - 1)
 8 IF(K1.NE.0.AND.NCF(NELE,K1).GT.0) THEN
 9 ISTOIC1 = ICKWRK(ICNU + (I-1)*MXSP + N1 − 1)
10 IF(K.NE.K1.AND.ISTOIC*ISTOIC1.LT.0) THEN
11 IFROM = K
12 ITO = K1
13 NAJ = ABS(ISTOIC)*NCF(NELE,IFROM)
14 NAK = ABS(ISTOIC1)*NCF(NELE,ITO)
15 AJK(IFROM,ITO) = AJK(IFROM,ITO)
16 + (ABS(Qfwd(I))+ABS(Qrev(I)))*NAJ*NAK/
(NAI(I))
17 ENDIF
18 ENDIF
19 ENDDO
20 ENDIF
21 ENDDO
22 ENDDO
```

Manuscript received Feb. 9, 2009, and revision received July 19, 2009.